Food & Function

ROYAL SOCIETY OF CHEMISTRY

PAPER

View Article Online
View Journal | View Issue

Cite this: *Food Funct.*, 2024, **15**, 8370

Miao sour soup alleviates DSS-induced colitis in mice: modulation of gut microbiota and intestinal barrier function†

Lincao Li, ‡[a,b] Haiyan Sun,‡[a] Lunbo Tan, ‡[c,d] Hui Guo,[a] Lisi He,[a] Jieyu Chen,[a] Shuting Chen,[a] Dong Liu,*[a] Mingjun Zhu *[b] and Zijun OuYang *[a,b]

Miao sour soup (MSS), a daily fermented food in Guizhou, China, is rich in microorganisms with various beneficial activities, including anti-inflammatory and antioxidant activities. However, the therapeutic effects of MSS on IBD remain unexplored. This study aimed to investigate the protective effect of MSS against colitis in mice. In this study, we examined the microbial community structure of MSS by metagenomic sequencing and also explored the protective effect of MSS on DSS-induced colitis in mice. We investigated the effects of MSS on intestinal inflammatory response and intestinal barrier function in mice. Finally, the changes in intestinal flora were analyzed based on the 16S rRNA gene sequencing results. Significantly, the experiment result shows that MSS ameliorated the severity of DSS-induced disease in mice by mitigating colitis-associated weight loss, reducing the disease activity index of IBD, alleviating colonic hemorrhagic lesions, increasing colon length, and improving colonic tissue damage. Moreover, MSS preserved intestinal barrier integrity and restored intestinal epithelial function in mice. Additionally, MSS modulated the structure and composition of the intestinal flora. Furthermore, MSS downregulated pro-inflammatory factors and attenuated the NF-κB p65 expression, thereby mitigating the inflammatory response. These findings highlight the protective effect of MSS against DSS-induced colitis, providing substantial scientific support for potential applications of MSS as a functional food.

Received 17th April 2024,
Accepted 14th June 2024

DOI: 10.1039/d4fo01794c

rsc.li/food-function

Introduction

Inflammatory bowel disease (IBD), is a group of chronic, non-specific, recurrent inflammatory diseases occurring in the colon and small intestine.[1] Symptoms include abdominal pain, diarrhea, rectal bleeding, and weight loss.[2] The pathogenesis of IBD primarily involves genetic susceptibility, environmental factors, epithelial barrier defects, dysregulated immune response, and intestinal flora disorders.[3] Global increases in IBD rates pose significant health and economic challenges.[4] Current treatment relies on medications,[5] but their high cost, temporary relief, and long-term side effects[6] emphasize the urgent need for safe, natural, and cost-effective measures to prevent and alleviate IBD.

Dietary therapy has emerged as an adjunctive IBD treatment, offering improved patient acceptance and therapeutic efficacy.[7] Fermented foods containing beneficial microorganisms have garnered attention as dietary supplements for preventing and treating IBD.[8] Numerous studies have confirmed that water kefir, kefir-fermented milk, barley, soybean mixtures, and fermented rice extract all exhibit protective effects against DSS-induced colitis in mice, which is the most widely used mouse model of IBD.[9–12] They mitigate inflammation, enhance intestinal barriers, and regulate gut flora. These findings highlight the potential of fermented foods as functional candidates for alleviating IBD symptoms.

Miao sour soup (MSS), a daily fermented food from Guizhou's Miao region in China,[13] is made by fermenting rice in a confined environment at 30–35 °C for 5 to 6 days.[14] This mixture contains organic acids (like lactic acid, citric acid, tartaric acid, and malic acid), as well as other nutrients, includ-

[a]*School of Food and Drug, Shenzhen Polytechnic University, 7098 Liuxian Avenue, Shenzhen 518055, China. E-mail: ouyangzijun@szpu.edu.cn, liudongsz@szpu.edu.cn*
[b]*School of Biology and Biological Engineering, Guangdong Key Laboratory of Fermentation and Enzyme Engineering, South China University of Technology, Guangzhou Higher Education Mega Center, Panyu, Guangzhou 510006, China. E-mail: mjzhu@scut.edu.cn*
[c]*Division of Vascular Medicine and Pharmacology, Department of Internal Medicine, Erasmus MC, Rotterdam, The Netherlands*
[d]*Women and Children's Hospital of Chongqing Medical University, Chongqing 401147, China*

†Electronic supplementary information (ESI) available. See DOI: https://doi.org/10.1039/d4fo01794c

‡These authors contributed equally to this work.

ing bacteriocins, amino acids, and vitamins, predominantly synthesized by lactic acid bacteria, acetic acid bacteria, and yeast through sugar fermentation.[15] MSS is also rich in short-chain fatty acids (SCFAs) such as acetic acid, propionic acid, and butyric acid, which energize the growth and reproduction of intestinal flora.[16] Studies highlight MSS's various human health benefits, including its antioxidant properties, protection against intestinal inflammation, and regulation of the gut microbial balance.[17–20] Long-term consumption of MSS aids appetite, digestion, and alleviates acute diarrhea.[14,17–20] Current MSS studies focus on improving flavour,[16] optimizing fermentation,[21–23] and bacterial flora screening,[24] but lacking IBD-related investigation.

In this study, we aimed to evaluate the effect of MSS on IBD-related colitis using DSS-induced colitis in mice and to elucidate the mechanism by analyzing metagenomics-sequencing of MSS alongside the physiological and pathological changes, and the alterations in fecal microbial composition after MSS treatment.

Materials and methods

Untargeted metabolomic analysis of MSS

MSS was prepared by washing cabbage, then precooking, draining, and fermenting it with noodle or rice soup and Laosuantang for 3–7 days, as reported previously.[14] MSS was filtered with a 0.22 μm filter, and a portion of the filtrate was diluted with LC-MS-grade water to achieve a methanol content of 50%. Let the mixture stand for 5 min, then vortexed, ultrasound for another 5 min, and centrifuged for 15 min (15 000*g*, 4 °C). Finally, the supernatant was collected for the metabolomics analysis. The LC-MS/MS analysis used a liquid chromatograph (LC-40D, SHIMADZU, Japan) coupled with a Q-TOF-MS/MS (Zeno TOF 7600, SCIEX, USA). Chromatographic conditions were as follows. Chromatographic column: ACQUITY UPLC BEH C18 (1.7 μm, 2.1 × 50 mm, Waters, USA). The injection volume was 5 μL, using a mobile phase was (A) 0.1% formic acid aqueous water solution and (B) 0.1% formic acid acetonitrile solution at the flow rate of 0.4 mL min^{-1} and column temperature of 40 °C. The gradient elution procedure was as follows: 0–1.5 min, A: 95%; 1.5–5.5 min, A: 70%; 5.5–10 min, A: 40%; 10–14.5 min, A: 2%; 14.5–20 min, A: 95%. The mass spectrometry conditions were as follows: electrospray ion source (ESI) positive and negative ion scanning modes were adopted, the gas temperature was maintained at 550 °C, and the curtain gas was set at 35 psi. The spray voltage was 5500 (+)/4500(−) V. Disclustering potential was set at 80 V, and collision energy at 10 V. TOF Mass range was set at *m*/*z* 50–1500 Da. All data were collected and processed using SCIEX software (OS3.0, USA).

Animal manipulation

All mouse experiments were approved by the Animal Ethics Review Committee of the South China University of Technology (permit no. 2022099). Female C57BL/6J mice were purchased from Guangdong GemPharmatech Biotechnology Co (Foshan, China), at 8 weeks old and housed in a 21 ± 2 °C controlled pathogen-free room under a 12 h-light/12 h-dark cycle with free access to food and water. After one week of acclimation, the mice were randomly divided into four groups (n = 6 mice per group), and performed intragastric administration every day for 7 days (Fig. S1A†): the normal control (NC) group with phosphate-buffered saline (PBS, Serviobo, China), the dextran sulfate sodium (DSS, molecular weight: 36–50 kDa, MP Biomedicals, USA) group with 2.5% of DSS, and the Miao sour soup (MSS) group (2.5% DSS + 100 μL per 10 g MSS) or the cell-free supernatant of MSS (CFS) group (2.5% DSS + 100 μL per 10 g CFS). During the experiment, the mice were weighed simultaneously every day. At the same time, mice feces were collected, and the characteristics of mice feces were recorded. The fecal occult blood kit (Baso, China) was used to test the blood status in mice. Disease activity index (DAI) scores were calculated according to the previous study's evaluation criteria (Table S1†).[25] After euthanizing the mice using isoflurane anesthesia, the whole intestinal tissue from the cecum to the anus was collected.

For tissue preparation, the intestinal tissue was photographed, and its length was measured. A portion of the colonic tissue was stored at −80 °C for subsequent analysis of experiments such as western blotting and quantitative real-time polymerase chain reaction (qRT-PCR). The remaining colonic tissue was fixed in a 4% paraformaldehyde solution for histological and related pathological experiments. The intestinal feces samples were collected and stored at −80 °C until further use.

Colonoscopy analysis. Following previously established protocols, a colonoscopy was performed on day 7 in mice using a microendoscope (TC200EN, STORZ, Germany).[26] Before the procedure, the mice underwent a 2 h fasting and were anesthetized. Hold the fur just above the anus of the mouse with one hand and the scope in the other hand. Carefully insert the endoscope into the rectum and find a clear view to photograph. The severity of colitis in mice was assessed using the mouse endoscopic index of colitis severity (MEICS score in Table S2†) according to the previous study.[26]

Mesenteric microcirculation analysis. Laser speckle contrast analysis (LASCA, RFLSI Pro, Reward, China) was used to detect the mesenteric vascular microcirculation in mice on day 8.[27] Before the examination, the mice were anesthetized and dissected after blood was drawn. After laparotomy, the intestines of the mice were gently removed with two cotton swabs and placed on the wet test paper. The cotton swabs were dipped in normal saline, the mice's intestines were spread and paved, while the hair on the intestines was removed. The laser light source of the instrument was pointed at the intestines of mice, and the images were recorded.

Intestinal permeability analysis. The intestinal permeability was evaluated by detecting the intestinal absorption of FITC-dextran into the bloodstream on day 8. As previously

described,[28] mice were fasted overnight for approximately 12 h and gavaged with 500 mg kg^{-1} FITC-Dextran (Sigma, USA). After 4 h, blood samples were collected before the sacrifice and centrifuged at 2000*g* for 20 min at 4 °C, and the serum samples were stored at −20 °C until analysis. The concentration of FITC-Dextran in serum was determined using a FITC-Dextran calibration curve (Exiation: 480 nm; Emission: 520 nm; Molecular Devices, USA).

Histological analysis. Fresh distal colon tissues were fixed overnight in 4% paraformaldehyde, then 4 μm thick slices were created through paraffin embedding. Haematoxylin and eosin (H&E, Servicebio, China) staining was used to assess the pathological lesions of the colon tissues, and the histological evaluation methods were referred to Table S3.†[29] The Alcian Blue-Periodic Acid Schiff (AB-PAS, Solarbio, China) staining,[30] was used for evaluating goblet cells in the colon tissues. The staining sections were imaged using a microscope (Leica, Germany). The number of goblet cells in the images was analysed using ImageJ software (NIH, USA).

Immunofluorescence. The expression of myeloperoxidase (MPO),[31] nuclear factor kappa B (NF-κB) p65 was analyzed by immunofluorescence.[32] Briefly, colonic slices were incubated with MPO primary antibody (Cat: AB208670, 1 : 200, Abcam, USA), NF-κB p65 primary antibody (Cat: 8242S, 1 : 200, Cell Signaling Technology, USA) overnight at 4 °C. Then the slides were incubated at room temperature for 1 h with fluorescent secondary antibody Goat Anti-Rabbit IgG HL (Alexa Fluor 594, Cat: AB150080, 1 : 200, Abcam, USA) and Goat Anti-Rabbit IgG (Alexa Fluor 488, Cat: L3016, 1 : 200, SAB, USA), respectively. Images were captured using confocal (ZEISS, Germany) and microscope (Leica, Germany), respectively. The fluorescence intensity of MPO was analyzed using ImageJ software (NIH, USA).

Apoptosis staining. The level of apoptosis in colonic tissue was detected using a terminal deoxynucleotidyl transferase-mediated dUTP nick end labeling (TUNEL) staining kit (Promega, USA) as described previously.[33] Cell nuclei were stained with DAPI (4′,6-diamidino-2-phenylindole, Solarbio, China) and images were obtained by fluorescence microscopy (Leica, Germany).

Quantitative real-time PCR

Total RNA was extracted from colon tissue following the procedure of the Eastep Super kit (Promega, USA) and quantified using a NanoPhotometer (NP80 Touch, Implen, Germany). The reverse transcription reaction system was prepared according to the instructions of the GoScript™ Reverse Transcription Mix, Oligo (dT) kit (Promega, USA). Amplification for reverse transcription was carried out using a PCR instrument (Biometra TAdvanced 96 SG, Analytik Jena, Germany) following these steps: annealing at 25 °C for 5 min for 1 cycle; extension at 40 °C for 60 min for 1 cycle, and deactivation at 70 °C for 15 min for 1 cycle. The reaction system was prepared according to the method of the GoTaq qPCR Master Mix kit (Promega, USA), and the real-time fluorescence quantitative PCR was performed using the PCR instrument (QuantStudio 7 Pro, Thermo Fisher Scientific, USA) according to the procedures of "Hold Stage, 95 °C for 10 min, 1 cycle; PCR Stage, 60 °C for 1 min, 40 cycles, fluorescence collection; melt curve stage, 95 °C for 15 s, 60 °C for 1 min, and 95 °C for 1 s, fluorescence collection". The mRNA expression levels were normalized to β-actin expression. The relative mRNA expression levels of each gene in the DSS, MSS and CFS groups were calculated by the $2^{-\Delta\Delta Ct}$ method with respect to the NC group.[34] The specific qPCR primers are shown in Table S4.†

Western blot

Colon tissue samples were weighed, homogenized, and lysed in RIPA buffer (Absin, China). Following 15 min of centrifugation (12 000*g*, 4 °C), the supernatants were collected, and protein concentrations were determined using the bicinchoninic acid (BCA) protein assay kit (Thermo Fisher Scientific, USA). The proteins separated by 8% SDS-PAGE were transferred to polyvinylidene difluoride (PVDF) membrane. After sealing with 5% skimmed milk, the membranes were incubated overnight at 4 °C with the following primary antibodies: E-cadherin, NF-κB p65, β-actin (Cat: 3195S, 8242S, 4970S, 1 : 500 dilution, Cell Signaling Technology, USA), Occludin, Claudin-1 (Cat: sc-133256, sc-166338, 1 : 500 dilution, Santa Cruz, USA), and Zonula occludens-1 (ZO-1, Cat: AF5145, 1 : 500 dilution, Affinity, China). Then, the corresponding secondary antibodies (1 : 1000 dilution, Cell Signaling Technology) were incubated for 1 h at room temperature. The blot images were captured by ChemiDoc MP imaging system (BIO-RAD, USA). The densitometry of immunoblots were quantified with ImageJ software (NIH, USA).

Analysis of MSS microbiota and fecal microbiota

The total DNA extracted from MSS samples was performed macro-genome sequencing using primers for amplification to generate a library. The library was sequenced on the Nova platform (Illumina, USA). The raw Illumina sequences were deposited to the NCBI sequence read archive with the project accession number PRJNA1048723. Taxonomic information was annotated using Kraken2 and Bracken pairs based on the Kraken2 virus database.

Total DNA from fecal samples was extracted, followed by the amplification of 16S rRNA primers 515F (5′-CCTAYG GGRBGCASCAG-3′) and 806R (5′-GGACTACNNGGGGTATCT AAT-3′) to prepare Illumina DNA libraries. Subsequently, sequencing was performed on the Illumina platform. The original Illumina sequences were saved into the NCBI Sequence Read Archive with the project accession number PRJNA1048719. These sequences were then analyzed for α-diversity, and principal coordinate analysis (PCoA)using QIIME2, PICRUSt respectively, and displayed using R software (Version 2.15.3). Species annotation was performed using QIIME2 software, and the annotation database is Silva Database. Linear discriminant analysis Effect Size (LEfSe)

analysis (LDA score threshold: 2) was used for the analysis of biomarkers within different groups. Correlation of microbial structure with alterations of colitis index was performed by Pearson correlation.

Short-chain fatty acids analysis in cecum contents

According to the method of short-chain fatty acids (SCFAs), about 50 mg of cecum samples were weighed, diluted to a suitable volume with 80% methanol, ground with steel balls, vortexed, and centrifuged (20 000*g*, 4 °C) for 15 min. 20 μL supernatant was taken into 1.5 mL centrifuge tube, 1-(3-dimethylaminopropyl)-3-ethylcarbodiimide (EDC) and 3-nitrophenylhydrazine (3-NPH) solution were added for derivation. Then, 500 μL of the initial mobile phase solution was added, vortexed, and 200 μL was taken into sample vial for LC-MS/MS detection and analysis. The chromatographic mass spectrometry condition parameters are as follows: vanquish liquid chromatograph (Thermo Fisher Scientific, USA); chromatographic column: Agilent Poroshell 120 EC-C18, (2.7 μm, 2.1 × 100 mm); column temperature: 40 °C; sample size: 2 μL; mobile phase: A: water, B: acetonitrile solution of methanol (1 : 1). The mass spectrum condition parameters are as follows: liquid chromatography tandem mass spectrometry (TSQ Altis, Thermo Fisher Scientific, USA); Multi-Reaction Monitoring (MRM); negative ion mode.

Non-targeted metabolomics analysis of mice serum

50 μL of serum and 250 μL of methanol were taken in centrifuge tubes, vortexed for 3 min, and then centrifuged at 4 °C, 12 000*g* for 10 minutes. After centrifugation, the supernatant was evaporated under nitrogen, and then 100 μL of methanol were added to the residue and vortexed for 3 min, sonicated for 3 min, and then centrifuged at 4 °C, 12 000*g* for 10 min. The supernatant was pipetted into a liquid phase vial for detection. The chromatographic conditions and mass spectrometry conditions were reported previously in untargeted metabolomic analysis of MSS.

Statistical analysis

All data were presented as mean ± SEM, and the statistical comparisons were analyzed in GraphPad Prism 9.0 software with a One-way ANOVA test except for body weight change and DAI. The body weight change and DAI were analyzed with Two-way ANOVA. The statistical significance was as follows: compared with NC group, #: $p < 0.05$, ##: $p < 0.01$, ###: $p < 0.001$, ####: $p < 0.0001$; compared with DSS group, *: $p < 0.05$, **: $p < 0.01$, ***: $p < 0.001$, ****: $p < 0.0001$.

Results

Microbial composition of MSS

Metagenomics-Sequencing results showed that the dominant phylum of MSS used in this study was Firmicutes (91.50 ± 0.20%) (Fig. 1A). Additionally, MSS contained Proteobacteria (4.35 ± 0.01%), Actinobacteria (3.81 ± 0.13%), and other phyla (0.34 ± 0.01%). At the family level (Fig. 1B), Lactobacillaceae (90.65 ± 0.20%) from the Firmicutes phylum, was the most abundant, followed by Acetobacteriaceae

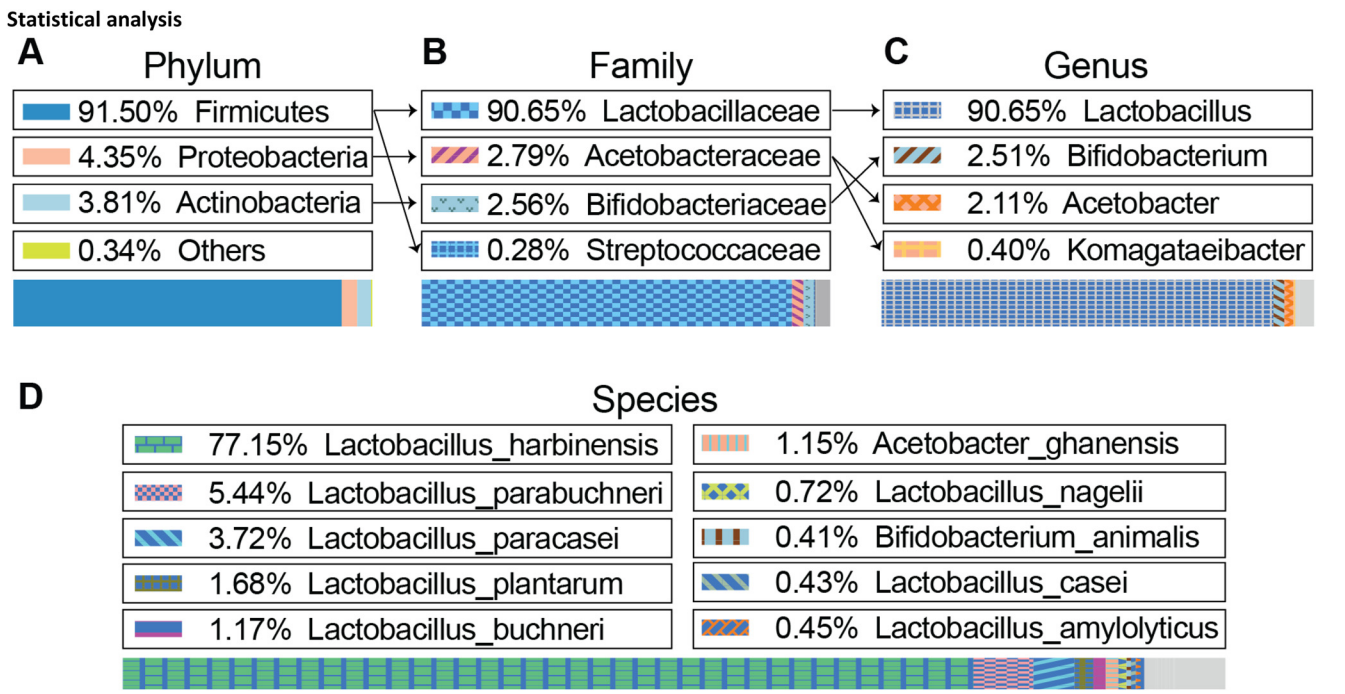

Fig. 1 The composition of microbiota in Miao sour soup (MSS). The relative ratios of microbiota in the MSS (n = 3), at the phylum (A), family (B), genus (C), and species levels (D), based on metagenomics data.

(2.79 ± 0.07%) from Proteobacteria, Bifidobacteriaceae (2.56 ± 0.11%) from Actinobacteria, and Streptococcaceae (0.28 ± 0.01%) from Firmicutes. Among genera (Fig. 1C), *Lactobacillus* (90.65 ± 0.20%) from the Lactobacillaceae, was the most abundant, followed by *Bifidobacterium* (2.51 ± 0.11%) from Bifidobacteriaceae, and *Acetobacter* (2.11 ± 0.06%) from Acetobacteriaceae. At the species level (Fig. 1D), the dominant species in the MSS were all from *Lactobacillus* genus, including *Lactobacillus harbinensis* (77.15 ± 0.91%), *Lactobacillus parabuchneri* (5.44 ± 0.59%), *Lactobacillus paracasei* (3.72 ± 0.07%), and *Lactobacillus plantarum* (1.68 ± 0.14%).

Identification of metabolites in MSS

The metabolites in MSS were identified through non-targeted metabolomics, and the total ion flow diagrams in both positive and negative ion modes are depicted in Fig. S2.† A total of 123 metabolites were identified across both ion modes, with specific information provided in Table S5.† The highest content was found to be 2-hydroxy-4-methylpentanoic acid, followed by 3-phenyllactic acid (Table 1). Moreover, nine amino acids were identified among the top 30 metabolites: norleucine, D-alloisoleucine, isoleucine, leucine, phenylalanine, proline, valine, tryptophan, and betaine.

MSS and CFS alleviated DSS-induced colitis in mice

After 7 days of induction (Fig. 2A), the body weight of the DSS group significantly decreased by 9.16% ± 1.97% from its baseline on day 0, compared to the NC group. In contrast, the MSS and CFS groups exhibited significantly less weight loss, with reductions of 4.55% ± 2.1% and 5.58% ± 2.24%, respectively, from their respective baselines on day 0. In the general diseased evaluation, the DAI score increased to 2.53 ± 0.40 in the DSS group. At the same time, MSS and CFS reduced the DAI score to 2.00 ± 0.36 and 1.78 ± 0.68, respectively, as compared to that of the DSS group (Fig. 2B). Specifically, colonoscopy revealed colonic wall lesions in mice from the DSS group (Fig. 2C). Yet, MSS and CFS interventions significantly ameliorated these lesions and reduced the Colonoscopy score (Fig. 2F). LASCA also showed mesenteric vascular microcirculation hyperaemia in the DSS group, which notably decreased following the MSS intervention compared to the DSS group of mice (Fig. S1B†). The colon length in the MSS group but not the CFS group was significantly longer than that in the DSS group and showed a similar shape to the NC group (Fig. 2E & G). The H&E staining (Fig. 2D) showed that in the NC group, the glands of the colonic tissue in mice were neatly aligned, with intact colonic mucosa, uniform crypt depth, and abundant goblet cells. In contrast, mice in the DSS group showed histopathological scores higher than those in the NC group (Fig. 2H), particularly exhibited disorganized colonic tissue

Table 1 The top30 metabolites information of MSS

No.	RT [min]	*m/z*	Metabolites name	Ontology
1	4.060	131.072	2-Hydroxy-4-methylpentanoic acid	Hydroxy fatty acids
2	4.444	165.056	3-Phenyllactic acid	Phenylpropanoic acids
3	1.382	121.065	Phenylacetaldehyde	Phenylacetaldehydes
4	7.864	415.212	Niranthin	Dibenzylbutane lignans
5	1.430	132.102	Norleucine	L-Alpha-amino acids
6	1.429	132.102	D-Alloisoleucine	Isoleucine and derivatives
7	1.431	132.102	Isoleucine	Isoleucine and derivatives
8	1.506	130.086	Leucine	Leucine and derivatives
9	9.905	149.023	4-Methylthio-2-oxobutanoic acid	Thia fatty acids
10	7.104	274.274	Lauryldiethanolamine	1,2-Aminoalcohols
11	1.682	164.072	Phenylalanine	Phenylalanine and derivatives
12	1.980	181.051	3-(4-Hydroxyphenyl)lactic acid	Phenylpropanoic acids
13	4.445	147.045	Cinnamic acid	Cinnamic acids
14	1.161	116.071	Proline	Proline and derivatives
15	1.201	118.086	Valine	Valine and derivatives
16	4.445	119.050	4-Vinylphenol	Styrenes
17	7.161	318.299	Phytosphingosine	1,3-Aminoalcohols
18	1.166	151.026	Oxypurinol	Xanthines
19	1.166	151.026	Xanthine	Xanthines
20	2.045	117.056	3-Hydroxyvaleric acid	Hydroxy fatty acids
21	1.980	203.082	Tryptophan	Indolyl carboxylic acids and derivatives
22	1.371	129.019	Itaconic acid	Organic acids
23	4.655	204.066	Indolelactic acid	Indolyl carboxylic acids and derivatives
24	16.18	118.086	Betaine	Alpha amino acids
25	9.902	279.159	Di-*n*-butyl phthalate	Benzoic acid esters
26	8.131	302.305	Tetradecyldiethanolamine	1,2-Aminoalcohols
27	7.161	230.247	*N,N*-Dimethyldodecylamine N-oxide	Long-chain alkyl amine oxides
28	5.969	163.039	4-Methylphthalic anhydride	Phthalic anhydrides
29	5.971	163.039	Umbelliferone	7-Hydroxycoumarins
30	7.396	593.129	[6-[2-(3,4-Dihydroxyphenyl)-8-hydroxy-4-oxochromen-7-yl] oxy-3,4,5-trihydroxyoxan-2-yl] methyl (*E*)-3-(4-hydroxyphenyl) prop-2-enoate	NA

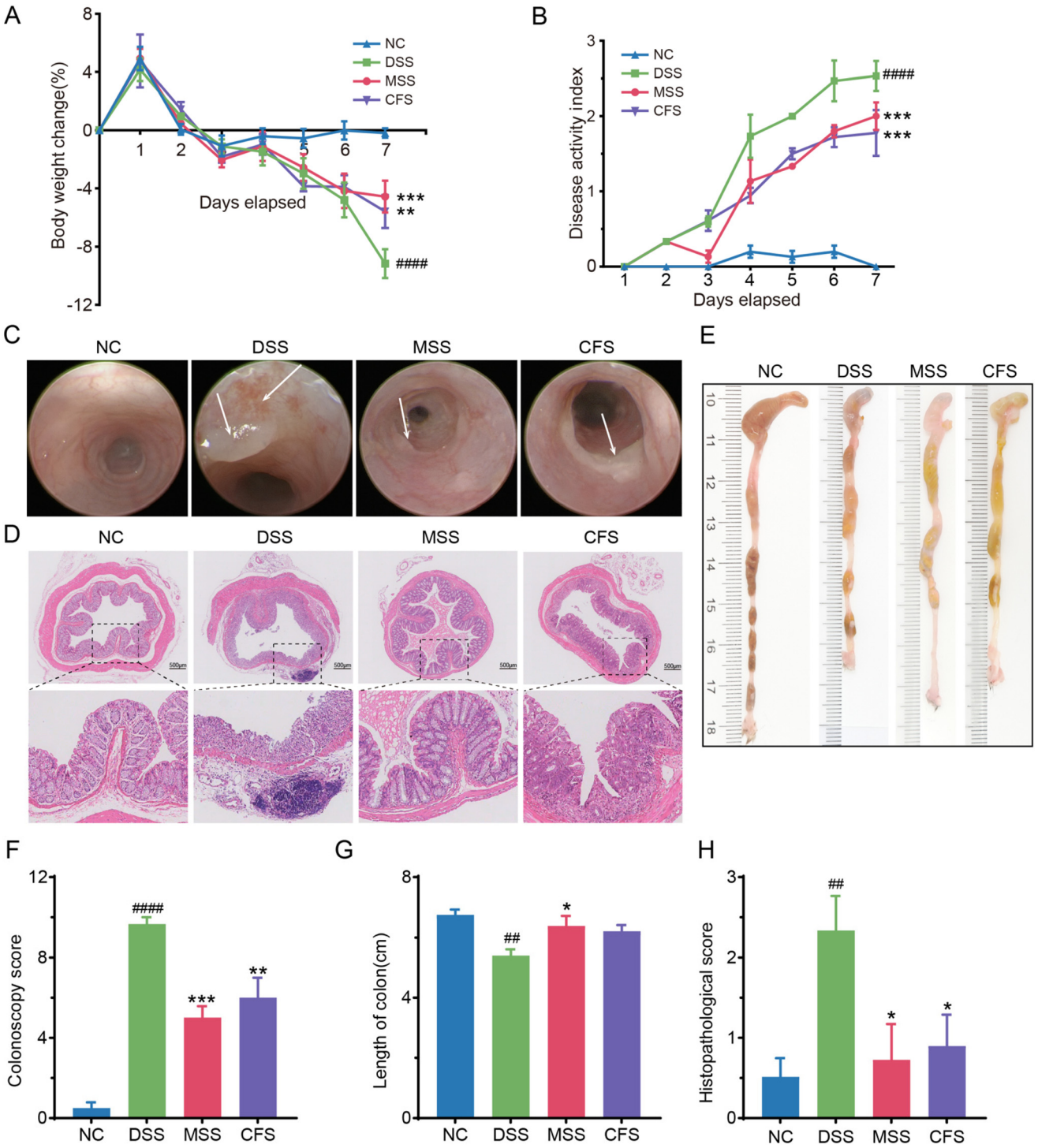

Fig. 2 MSS and CFS ameliorated DSS-induced colitis in mice. (A) Percentage change of body weight from baseline (day 0) during the treatment. (B) Disease activity index. (C) Representative images of electronic colonoscopy. (D) Representative images of H&E-stained colonic tissue. (E) Representative images of colons. (F) Colonoscopy score based on electronic colonoscopy, $n = 3$. (G) Statistical analysis of colon length, $n = 6$. (H) Histopathological scores of the colon tissues based on H&E staining, $n = 6$. Data are shown as mean ± SEM, significant differences to NC group are denoted by, #: $p < 0.05$, ##: $p < 0.01$, ####: $p < 0.0001$; significant differences to DSS group are denoted by, *: $p < 0.05$, **: $p < 0.01$, ***: $p < 0.001$ and ****: $p < 0.0001$.

glands, significantly reduced crypts and goblet cells, infiltration of inflammatory cells, and the damaged intestinal mucosa (Fig. 2D). After the treatment with MSS and CFS, these histopathological changes were reduced, and the score was returned to the level observed in the NC group (Fig. 2H).

MSS and CFS attenuated DSS-induced colonic inflammation

MPO content is positively correlated with IBD disease severity.[35] Immunofluorescence analysis showed that the MPO intensity was significantly higher than that of the NC group after DSS induction (Fig. 3A and B). Following MSS and CFS interventions (Fig. 3A and B), the MPO intensity decreased significantly ($p < 0.001$ and $p < 0.01$, respectively), with MSS

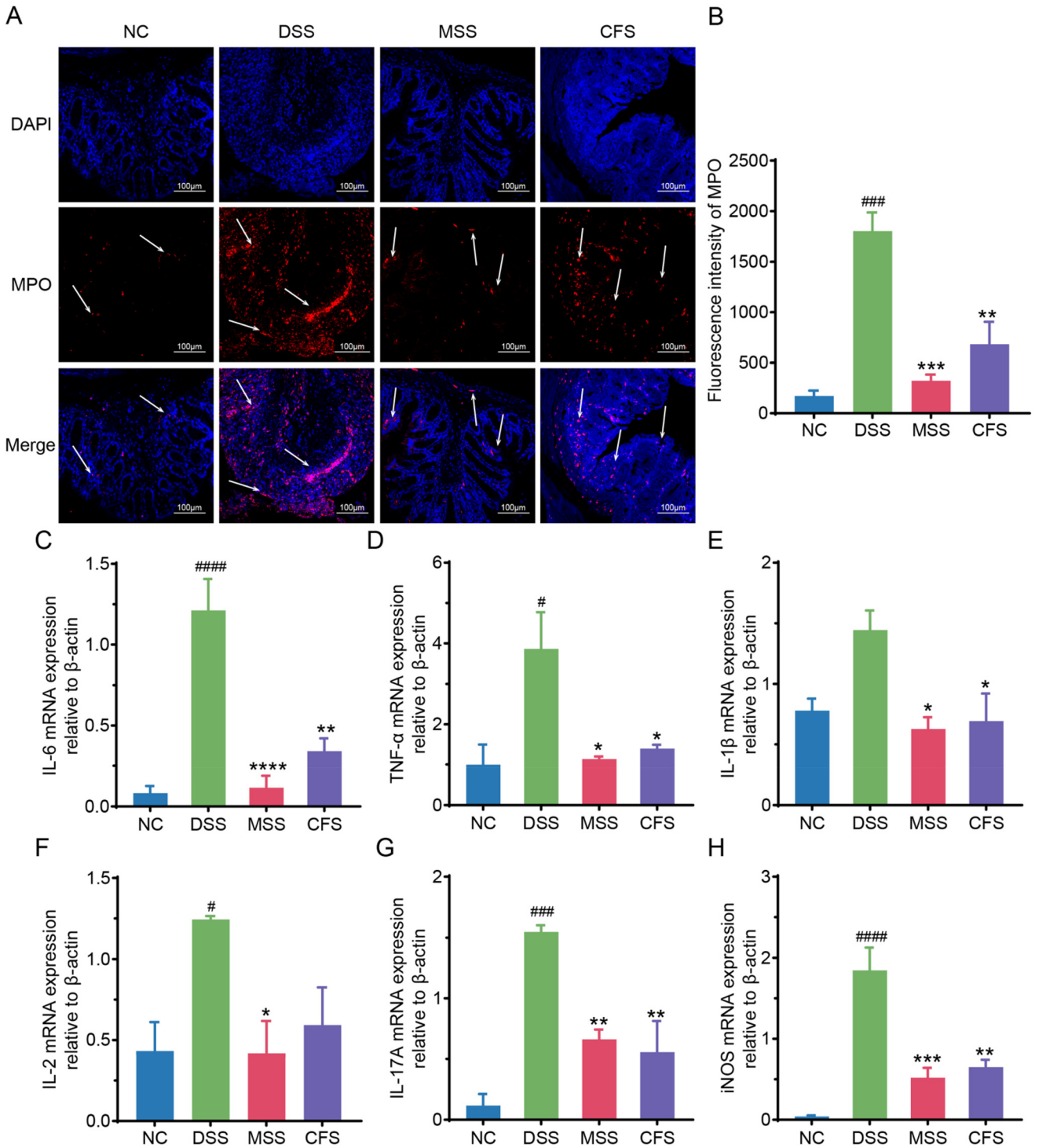

Fig. 3 MSS and CFS attenuated DSS-induced intestinal inflammatory response. Representative immunofluorescence images of MPO in colonic tissue (A) and quantitative analysis (B). The mRNA expression levels of IL-6, TNF-α, IL-1β, IL-2, IL-17A, and iNOS, respectively (C–H). Data were shown as mean ± SEM, $n = 6$. Significant differences to NC group are denoted by, #: $p < 0.05$, ###: $p < 0.001$; significant differences to DSS are denoted by, *: $p < 0.05$ and **: $p < 0.01$, ***: $p < 0.001$, ****: $p < 0.0001$. MPO: myeloperoxidase, IL-6: interleukin-6, TNF-α: tumor necrosis factor-alpha, IL-1β: interleukin-1β, IL-2: interleukin-2, IL-17A: interleukin-17A, iNOS: inducible nitric oxide synthase.

capable of restoring the MPO intensity to the level of the NC group. Additionally, mRNA levels of IL-6 (interleukin-6), TNF-α (tumor necrosis factor-alpha), IL-1β (interleukin-1β), IL-2 (interleukin-2), IL-17A (interleukin-17A), and iNOS (inducible nitric oxide synthase) were higher in DSS group colons compared to NC group. However, significance was not observed in IL-1β (Fig. 3C–H). After MSS and CFS intervention, the levels of these proinflammatory cytokines were decreased.

MSS and CFS restored intestinal barrier function in DSS induced colitis mice

As intestinal barrier dysfunction has been widely accepted as a distinctive feature of colitis, we then use serum FITC-Dextran leakage to evaluate the intestinal epithelial barrier. Briefly, the concentration of the FITC-Dextran was usually detected after 4 hours of FITC-Dextran intragastric administration, which can reflect the integrity of the intestinal epithelial barrier. Serum FITC-Dextran concentration significantly increased ($p < 0.05$) in the DSS group. However, it was obviously decreased ($p < 0.05$) in the MSS and CFS group (Fig. 4A), indicating that MSS and CFS could reduce intestinal permeability. TUNEL staining also showed that TUNEL signal and apoptosis rate ($p < 0.001$ and $p < 0.01$, respectively) were reduced after the MSS and CFS interventions, as compared to that in the DSS group (Fig. 4B & D). The AB-PAS staining showed that (Fig. 4C & E), in the NC group, the well-organized goblet cells exhibited the mucin (blue and purple stained) positive stating in the mucus layer. In contrast, the DSS group showed severe mucus layer disruption and a reduced number of goblet cells. After MSS treatment, this disruption was reversed, and the number of goblet cells was also increased, but there was no significant difference compared to the DSS group in the CFS group (Fig. 4C & E).

Overall, when comparing MSS and CFS, MSS showed a more effective treatment of DSS-induced colitis in mice. Interestingly, consistent with the AB-PAS staining results, the mRNA level of mucin 2 (MUC2) was significantly decreased in the DSS group, which was reversed after MSS intervention (Fig. S3A†). The protein expression levels of intestinal barrier function makers (E-cadherin, ZO-1, Claudin-1, and Occludin) were detected by western blotting (Fig. S3B–S3F†). Compared with the NC group, the levels of all the above proteins were significantly reduced in the DSS group of mice. However, all these levels were restored after the MSS intervention.

MSS modulated gut microbial composition in colitis mice

The DSS group had the lowest Chao1 index (an indicator of species richness) of 136.91 ± 37.70, followed by 175.44 ± 65.61 in the MSS group, and the highest Chao1 index was 367.89 ± 54.92 in the NC group (Fig. 5A). PCoA analysis based on Bray–Curtis showed that all groups were distinctly separated from each other (Fig. 5B). The analysis of intestinal flora composition showed that the flora changed at the phylum level after DSS induction (Fig. 5C). Verrucomicrobiota decreased significantly, along with Firmicutes, while Proteobacteria increased significantly (Fig. 5E, F and S4A†). However, after MSS intervention, there was a substantial recovery in the abundance of Firmicutes, Lachnospiraceae, and Peptococcaceae (Fig. 5E, S4B & S4D†) and a decrease in Proteobacteria (Fig. 5F). Moreover, DSS significantly increased the relative abundance of Enterobacteriaceae, Deferribacteraceae, and Enterococcaceae (Fig. S4E–S4G†). The abundance of these families was reduced after the intervention of MSS (Fig. S4E–S4G†). At the genus level, the relative abundance of *Bifidobacterium*, *Lachnospiraceae NK4A136*, and *Akkermansia* decreased in the DSS group (Fig. 5G–I). After MSS intervention, the relative abundance of the above genera was increased, while the relative abundance of *Enterococcus* significantly decreased (Fig. 5G–J). In addition, MSS significantly improved DSS-suppressed levels of propionic acid, butyric acid, isobutyric acid, and isovaleric acid in the cecum (Fig. S5†).

MSS's effect on mice's gut microbiota was further investigated using LEfSe analysis, and the results are presented as a LDA score. High scores were observed for *Rikenella* and *Eubacterium coprostanoligenes group* in the NC group, Eukaryota, Erysipelotrichaceae, and Ruminococcaceae in the MSS group, and *Rodentibacter-heylii*, Pasteurellaceae, and Pasteurellales in the DSS group (Fig. 6A).

The correlation coefficients between gut bacteria at the genus level and colitis-related indicators (common parameters, intestinal barrier, SCFAs, and inflammation) were calculated to investigate further the potential role of MSS-regulated gut microbiota in colitis. As shown in Fig. 6B, the clustering results showed that the bacteria genera can be divided into two groups. The abundance of most genera in Group 1 increased in the MSS group, showing a negative correlation with DAI, FITC-Dextran, and inflammatory parameters (TNF-α, IL-17, IL-6, IL-1β, IL-2) but showed a positive correlation with weight change, colon length, intestinal barrier (Goblet cells, E-cadherin, Claudin-1), and SCFAs (Acetic acid, Propionic acid, Butyric acid, Isobutyric acid, and Valeric acid). In contrast, the abundance of Group 2 genera increased in the DSS group, showing a positive correlation with DAI, FITC-Dextran, and inflammatory parameters and a negative correlation with weight change, colon length, intestinal barrier, and SCFAs.

MSS restored the serum metabolic profile in mice

Metabolic changes are crucial indicators of intestinal disease. During inflammation, the metabolic profile shifts, affecting host pathways. Using non-targeted metabolomics, we identified critical changes in mice serum. PCA and PLS-DA analyses (Fig. S6A and S6B†) distinguish DSS and NC groups, with MSS in between, closer to NC group. Colitis significantly alters mouse serum metabolism, but MSS intervention helps normalize it. We found 36 metabolites between DSS and MSS groups, highlighted in a heatmap (Fig. S6C†) and detailed in Table S6.†

KEGG analysis shows key pathways altered between DSS and MSS groups, including glycine, serine, and threonine metabolism, biosynthesis of unsaturated fatty acids, and primary bile acid biosynthesis (Fig. S6D†).

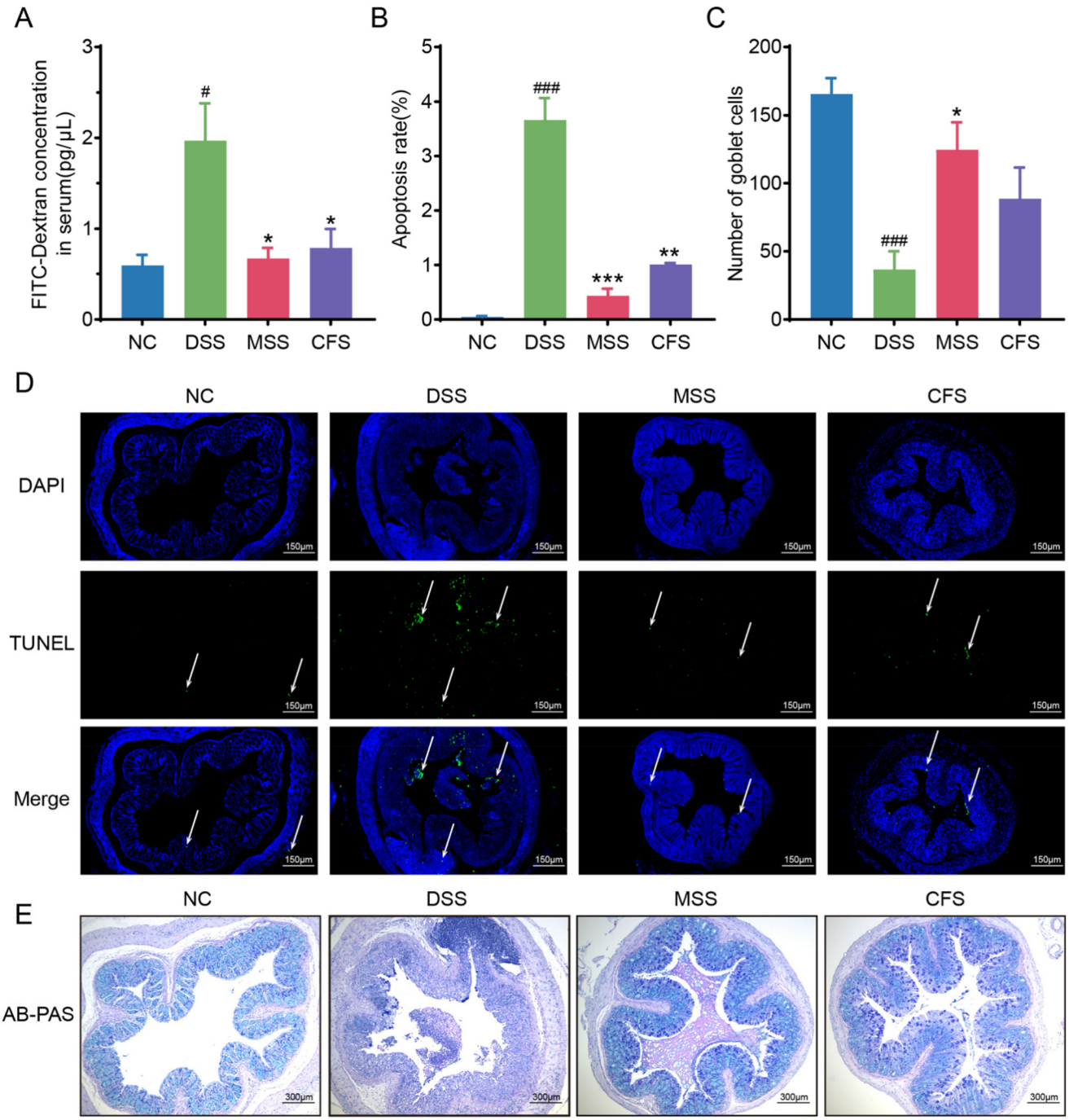

Fig. 4 MSS and CFS repaired the gut barrier in DSS-induced colitis mice. (A) Concentration of FITC-Dextran in serum, $n = 4$. (B) Quantitative analysis of apoptosis rate according to TUNEL staining, $n = 6$. (C) Count of goblet cells, $n = 6$. (D) Representative images of TUNEL staining in colonic tissue. (E) Representative images of colonic tissue stained with AB-PAS. Data are shown as mean ± SEM. Significant differences to NC group are denoted by, #: $p < 0.05$, ###: $p < 0.001$; significant differences to DSS group are denoted by, *: $p < 0.05$, **: $p < 0.01$ and ***: $p < 0.001$.

MSS attenuated DSS-induced colitis through NF-kB pathway

Metabolomics analysis found that 16 of the top 50 metabolites in MSS appeared in the serum of mice after the intervention MSS, as shown in the Venn diagram (Fig. 7A). Interestingly, we performed KEGG signaling pathway enrichment analysis for these 16 shared metabolites and found that the NF-κB pathway ranked among the top 5 metabolite enrichment analyses (Fig. 7B). Furthermore, this alteration was further confirmed in the colon tissue, where NF-κB p65 was found to be significantly increased in the cytoplasm and nucleus of the DSS group and decreased in the MSS group (Fig. 7C). Western blot

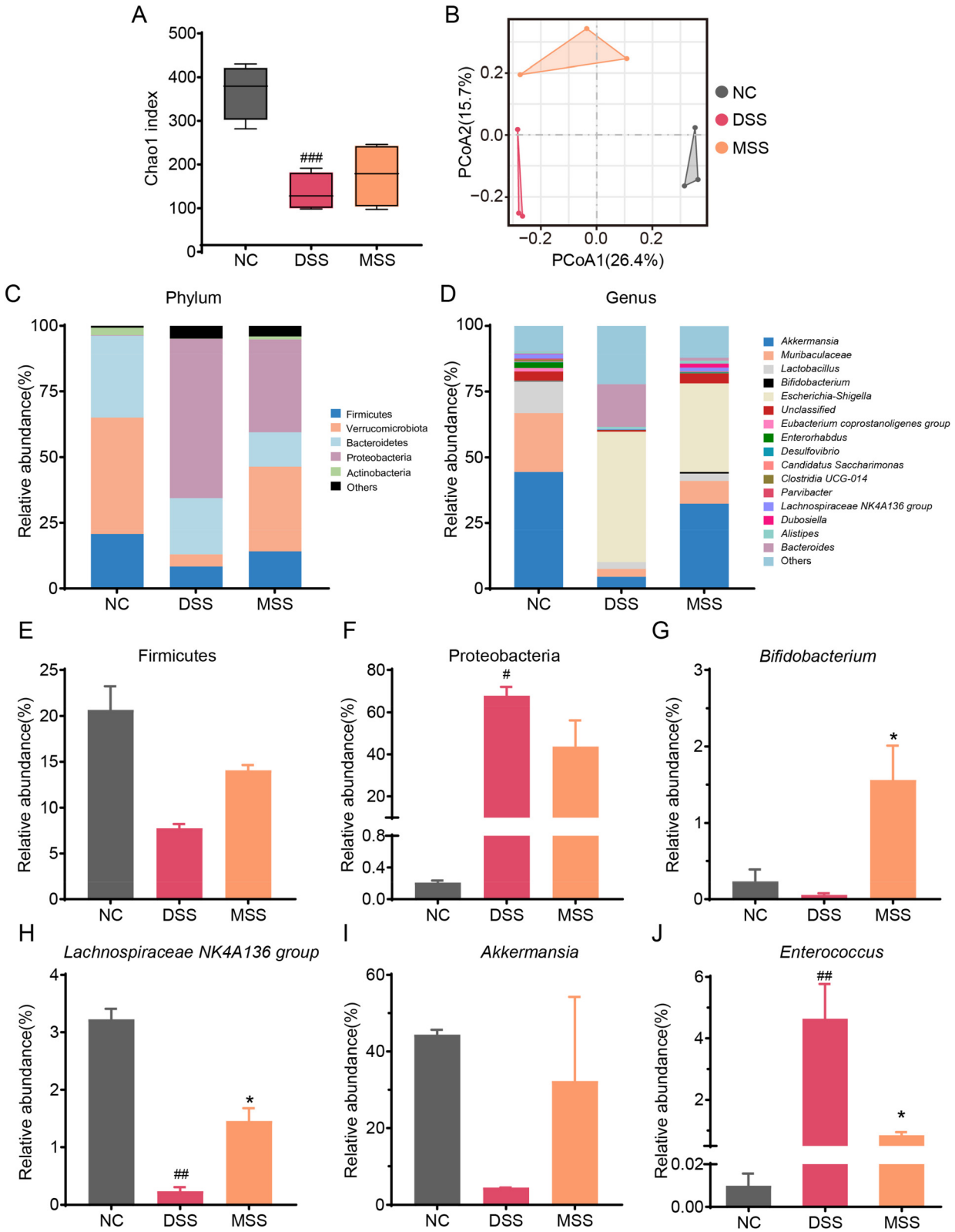

Fig. 5 MSS modulated gut microbiota composition in DSS-induced colitis. (A) Chao1 index. (B) PCoA analysis. (C) Composition of gut microbiota at the phylum level. (D) Composition of gut microbiota at the genus level. (E) Relative abundance of Firmicutes. (F) Relative abundance of Proteobacteria. (G) Relative abundance of *Bifidobacterium*. (H) Relative abundance of *Lachnospiraceae NK4A136* group. (I) Relative abundance of *Akkermansia*; (J) relative abundance of *Enterococcus*. Data are shown as mean ± SEM. Significant differences to NC group are denoted by, #: $p < 0.05$, ##: $p < 0.01$, ###: $p < 0.001$; significant difference to DSS group is denoted by, *: $p < 0.05$.

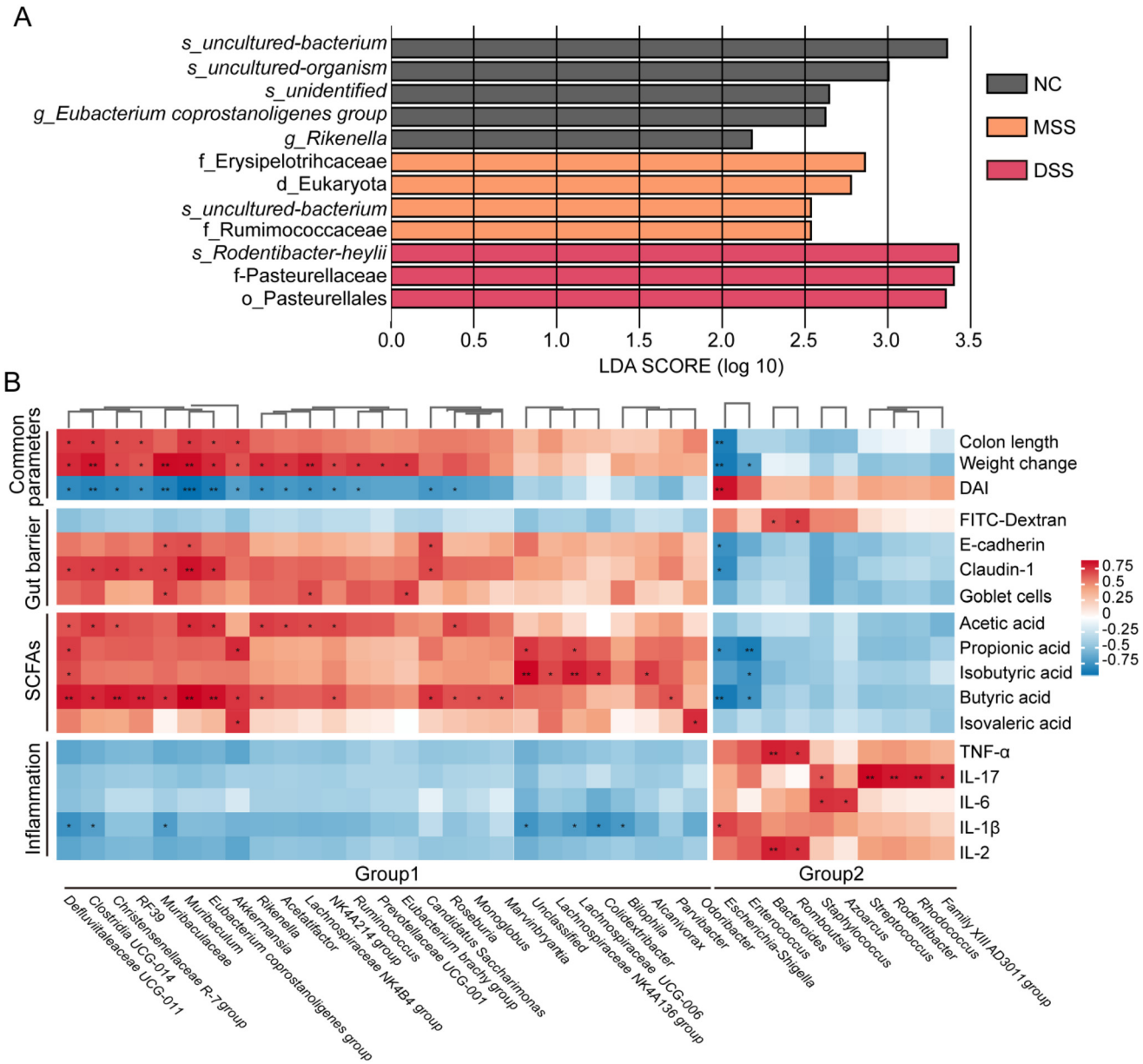

Fig. 6 LEfSe analysis of gut microbiota and correlation analysis of intestinal bacteria genus level and colitis. (A) LDA score of gut microbiota. (B) Heatmap of Pearson's correlation between the bacteria at the genus level and UC-related parameters. Groups 1 and 2 are generated based on the clustering results of the gut microbiota. *: $p < 0.05$, **: $p < 0.01$. LDA: linear discriminant analysis.

analysis also confirmed DSS-induced p65 expression, which was decreased by MSS treatment (Fig. 7D and E).

Discussion

The DSS-induced colitis model, known for its rapidity, controllability, and reproducibility, is widely used in mouse colitis studies.[36] In this study, mice induced with acute colitis by consuming 2.5% DSS in their drinking water for seven consecutive days exhibited various clinical symptoms, including weight loss, diarrhea, blood in the stool, colonic fibrin exudation, colon shortening, mucosal edema, inflammatory cell infiltration, and goblet cell loss. These findings align with previous studies.[36,37]

Numerous studies have reported that intestinal flora plays a crucia role in the pathogenesis of IBD.[38] Diet can shape gut flora, potentially alleviating related diseases, including IBD.[39,40] IBD patients and DSS-induced colitis mice show notably reduced microbial diversity compared to healthy controls.[41] The Firmicutes, known for producing beneficial butyric acid, decreased in IBD patients, whereas the Proteobacteria, associated with various pathogens, showed an increase in IBD patients.[42] In the present study, DSS-induced gut microbiota

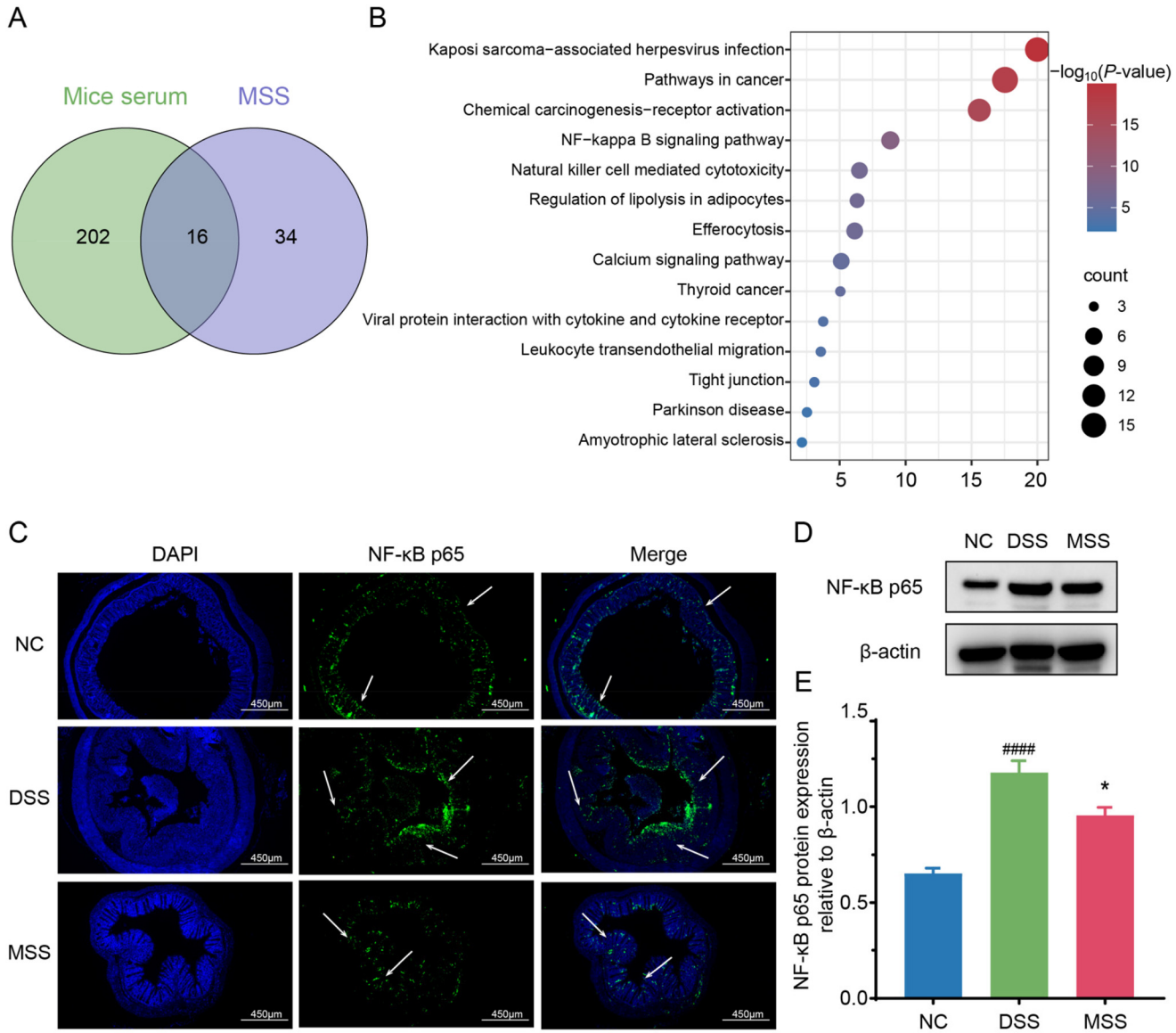

Fig. 7 The mechanism of MSS attenuated DSS-induced colitis. (A) Venn diagram analysis of metabolites in mice serum and the top 50 metabolites in MSS supernatant. (B) Signaling pathway enrichment analysis of shared metabolites. (C) Representative immunofluorescence images of NF-κB p65. The protein expression level (D) and quantitative analysis (E) of NF-κB p65. Data are presented as mean ± SEM. Significant difference compared to the NC group is denoted by ###: $p < 0.001$; significant difference compared to DSS group is denoted by *: $p < 0.05$.

increased genera known to worsen inflammation, which is aligned with prior studies: *Desulfovibrio*, belonging to the Proteobacteria, produces H_2S, contributing to intestinal inflammation;[43] *Mucispirillum* is recognized as a mucus-parasitic organism implicated in causing disease and tends to increase during colitis-related inflammation.[44] *Bacteroides* is associated with colitis in IBD-susceptible mouse models;[45] *Enterococcus* has been shown to increase the risk of intestinal inflammation;[46] *Escherichia–Shigella* promotes worsening of IBD;[9] The susceptibility of *Parasutterella* to enterocolitis and sepsis has detrimental effects on intestinal health.[47]

Our study found that MSS is predominantly composed of *Lactobacillus* (90.56%) and *Bifidobacterium* (2.51%). These genera include probiotics known for anti-inflammatory and gut-protective effects.[48] Interestingly, the present study showed that MSS treatment not only can reduce the abundance of DSS-induced pathogenic bacteria, but also increased the richness of microbial diversity in colitis mice, and mainly reduced the percentage of Proteobacteria in mice. Moreover, the MSS intervention restored the abundance of Verrucomicrobiota in colitis mice, which provide energy and nutrients and produce SCFAs, among other things, which are essential for intestinal health and immune system regulation.[49]

SCFAs, products of dietary fiber fermentation, are beneficial to hosts.[50] IBD patients often lack SCFA-producing bacteria and show reduced SCFAs levels.[51] After DSS induction, mice in

their cecum exhibited significantly lower acetic, propionic, and butyric acid levels.[52] However, after MSS intervention, a significant increase in SCFAs in the cecum of mice likely resulted from the enhancement of SCFAs-producing intestinal flora, represented by genera such as *Lachnospiraceae NK4A136* group,[53] *Akkermansia*,[54] *Bifidobacterium*,[55] and *Dubosiella*,[56] known for their roles in modulating immunity and producing beneficial acids. This suggests potential protective effects of MSS treatment against colitis and inflammatory diseases.

Intestinal barrier dysfunction reflects IBD development,[3] which correlates with inflammation. In our study, DSS-induced damage increased intestinal permeability and reduced crucial barrier maintenance proteins (E-cadherin, ZO-1, Occludin, Claudin-1).[57,58] Elevated pro-inflammatory factors (IL-1β, IL-6, TNF-α)[59] and MPO (a biomarker for gut inflammation in IBD)[60] in DSS-induced colitis contribute to inflammation. Moreover, excess iNOS induces NO production and inflammation.[61] Interestingly, the cell-free supernatant of MSS also ameliorates DSS-induced colitis by restoring the barrier function and reducing these DSS-induced pro-inflammatory factors, albeit with less effect compared to MSS, suggesting that the fermentation nutrients of MSS play an important role in the intervention's effectiveness. However, the complete product with microorganisms, MSS, demonstrates a superior effect.

The potential mechanism of MSS treatment on DSS-induced colitis may involve the NF-κB pathway, which regulates the transcription of various pro-inflammatory factors and could in turn aggravate inflammation.[9] In our study, non-targeted metabolomics analysis on both serum with MSS treatment and MSS identified 16 shared metabolites. Interestingly, NF-κB stood at the top of the pathway enrichment list. Moreover, we confirmed that the expression of NF-κB p65 increased in the DSS-induced colon and decreased with MSS treatment. Thus, the NF-κB pathway appears to be the most relevant pathway under MSS intervention in DSS-induced colitis. This suggests that MSS may reduce inflammation by acting on the NF-κB pathway, thus treating colitis.

Conclusions

In this study, MSS demonstrates efficacy in lessening DSS-induced colon damage *via* NF-κB pathway, reducing inflammation, and restoring intestinal health. This study underscores its potential as a functional food for IBD. Further research is required to identify the specific bioactive components responsible for alleviating IBD symptoms, aiding the development of tailored foods for IBD patients.

Data availability

The raw Illumina sequences of MSS microbiota were deposited to the NCBI sequence read archive with the project accession number PRJNA1048723. The original Illumina sequences of fecal microbiota were saved into the NCBI Sequence Read Archive with the project accession number PRJNA1048719. Processed data files are included as supplementary excel files with this article.

Author contributions

L. Li, H. Sun, and L. Tan: conceptualization, methodology, investigation, visualization, writing – original draft, preparation. H. Guo, L. He, J. Chen, and S. Chen: investigation, methodology, visualization. D. Liu and M. Zhu: conceptualization, methodology, writing – review & editing, supervision. Z. OY: conceptualization, methodology, investigation, visualization, writing – original draft, review & editing, supervision.

Conflicts of interest

The authors declare that there are no conflicts of interest.

Acknowledgements

This work was financially supported by the Characteristic Innovation Project of Guangdong Provincial Education Department (No. 2023KTSCX320); Shenzhen Science and Technology Program (No. 20231126130044001, No. 20220814205518001, No. 20230731094501002); Innovation Platform and Innovation Team of Guangdong Education Department (No. 2021CJPT014, 2021KCXTD069).

References

1 R. Ungaro, S. Mehandru, P. B. Allen, L. Peyrin-Biroulet and J.-F. Colombel, Ulcerative colitis, *Lancet*, 2017, **389**, 1756–1770.
2 M. F. Neurath, Targeting immune cell circuits and trafficking in inflammatory bowel disease, *Nat. Immunol.*, 2019, **20**, 970–979.
3 S. M. Vindigni, T. L. Zisman, D. L. Suskind and C. J. Damman, The intestinal microbiome, barrier function, and immune system in inflammatory bowel disease: a tripartite pathophysiological circuit with implications for new therapeutic directions, *Ther. Adv. Gastroenterol.*, 2016, **9**, 606–625.
4 V. Jairath and B. G. Feagan, Global burden of inflammatory bowel disease, *Lancet Gastroenterol Hepatol.*, 2020, **5**, 2–3.
5 A. Ali Sohrabpour, R. Malekzadeh and A. Keshavarzian, Current Therapeutic Approaches in Inflammatory Bowel Disease, *Curr. Pharm. Des.*, 2010, **16**, 3668–3683.
6 B. Gros and G. G. Kaplan, Ulcerative Colitis in Adults: A Review, *J. Am. Med. Assoc.*, 2023, **330**, 951–965.
7 E. A. Reznikov and D. L. Suskind, Current Nutritional Therapies in Inflammatory Bowel Disease: Improving

Clinical Remission Rates and Sustainability of Long-Term Dietary Therapies, *Nutrients*, 2023, **15**, 688.

8 N. Şanlier, B. B. Gökcen and A. C. Sezgin, Health benefits of fermented foods, *Crit. Rev. Food Sci. Nutr.*, 2017, **59**, 506–527.

9 Z. Ye, X. Yang, B. Deng, Z. Liao, X. Fang and J. Wang, Prevention of DSS-induced colitis in mice with water kefir microbiota via anti-inflammatory and microbiota-balancing activity, *Food Funct.*, 2023, **14**, 6813–6827.

10 K. Nascimento da Silva, A. G. Fávero, W. Ribeiro, C. M. Ferreira, P. Sartorelli, L. Cardili, C. S. Bogsan, J. N. Bertaglia Pereira, R. de Cássia Sinigaglia, A. Cristina de Moraes Malinverni, A. P. Ribeiro Paiotti, S. J. Miszputen and O. Ambrogini-Júnior, Effects of kefir fermented milk beverage on sodium dextran sulfate (DSS)-induced colitis in rats, *Heliyon*, 2023, **9**, e12707.

11 J. K. Woo, S. Choi, J. H. Kang, D. E. Kim, B.-S. Hurh, J. E. Jeon, S. Y. Kim and S. H. Oh, Fermented barley and soybean (BS) mixture enhances intestinal barrier function in dextran sulfate sodium (DSS)-induced colitis mouse model, *BMC Complementary Altern. Med.*, 2016, **16**, 498.

12 W. S. Oh, J. C. Jung, Y. M. Choi, J. Y. Mun, S. K. Ku and C. H. Song, Protective effects of fermented rice extract on ulcerative colitis induced by dextran sodium sulfate in mice, *Food Sci. Nutr.*, 2020, **8**, 1718–1728.

13 D. Li, F. Duan, Q. Tian, D. Zhong, X. Wang and L. Jia, Physiochemical, microbiological and flavor characteristics of traditional Chinese fermented food Kaili Red Sour Soup, *LWT*, 2021, **142**, 110933.

14 C. Wang, Q. Zhang, L. He and C. Li, Determination of the microbial communities of Guizhou Suantang, a traditional Chinese fermented sour soup, and correlation between the identified microorganisms and volatile compounds, *Food Res. Int.*, 2020, **138**, 109820.

15 N. Liu, X. Li, Y. Hu, L. Qin, A. Bao, W. Qin and S. Miao, Effects of Lentilactobacillus buchneri and Kazachstania bulderi on the Quality and Flavor of Guizhou Fermented Red Sour Soup, *Foods*, 2023, **12**, 3753.

16 W. Wu, X. Wang, P. Hu, Y. Zhang, J. Li, J. Jiang, R. Zheng and L. Zhang, Research on flavor characteristics of beef cooked in tomato sour soup by gas chromatography-ion mobility spectrometry and electronic nose, *LWT*, 2023, **179**, 114646.

17 P. Liu, Y. Xu, J. Ye, J. Tan, J. Hou, Y. Wang, J. Li, W. Cui, S. Wang and Q. Zhao, Qingre Huazhuo Jiangsuan Decoction promotes autophagy by inhibiting PI3K/AKT/mTOR signaling pathway to relieve acute gouty arthritis, *J. Ethnopharmacol.*, 2023, **302**, 115875.

18 Q. Zhou, Z. Qu, N. Wang, H. Liu, H. Yang and H. Wang, Miao sour soup influences serum lipid via regulation of high–fat diet–induced intestinal flora in obese rats, *Food Sci. Nutr.*, 2022, **11**, 2232–2242.

19 H. Yang, J. Xie, N. Wang, Q. Zhou, Y. Lu, Z. Qu and H. Wang, Effects of Miao sour soup on hyperlipidemia in high–fat diet–induced obese rats via the AMPK signaling pathway, *Food Sci. Nutr.*, 2021, **9**, 4266–4277.

20 S. Cong, Z. Li, L. Yu, Y. Liu, Y. Hu, Y. Bi and M. Cheng, Integrative proteomic and lipidomic analysis of Kaili Sour Soup-mediated attenuation of high-fat diet-induced nonalcoholic fatty liver disease in a rat model, *Nutr. Metab.*, 2021, **18**, 1–12.

21 D. Feixia, L. Ya, L. Dafei, Z. Dingjiang, H. Guiping, W. Zeliang and J. Lirong, Kaili Red sour soup: Correlations in composition/microbial metabolism and flavor profile during post-fermentation, *Food Chem.*, 2024, **435**, 137602.

22 N. Liu, Y. Hu, L. Qin, A. Bao, W. Qin and S. Miao, Flavor and quality characteristics of Guizhou red sour soup prepared by different artificially fortified fermentation methods, *LWT*, 2023, **186**, 115247.

23 C. Li, Q. Zhang, C. Wang, L. He, H. Tao, X. Zeng and Y. Dai, Effect of Starters on Quality Characteristics of Hongsuantang, a Chinese Traditional Sour Soup, *Fermentation*, 2022, **8**, 589.

24 K. Xiong, F. Han, Z. Wang, M. Du, Y. Chen, Y. Tang and Z. Wang, Screening of dominant strains in red sour soup from Miao nationality and the optimization of inoculating fermentation conditions, *Food Sci. Nutr.*, 2020, **9**, 261–271.

25 J. Liu, J. Cai, P. Fan, X. Dong, N. Zhang, J. Tai and Y. Cao, Salidroside alleviates dextran sulfate sodium-induced colitis in mice by modulating the gut microbiota, *Food Funct.*, 2023, **14**, 7506–7519.

26 C. Becker, M. C. Fantini and M. F. Neurath, High resolution colonoscopy in live mice, *Nat. Protoc.*, 2007, **1**, 2900–2904.

27 D. Kocsis, S. Horváth, Á. Kemény, Z. Varga-Medveczky, C. Pongor, R. Molnár, A. Mihály, D. Farkas, B. M. Naszlady, A. Fülöp, A. Horváth, B. Rózsa, E. Pintér, R. Gyulai and F. Erdő, Drug Delivery through the Psoriatic Epidermal Barrier—A "Skin-On-A-Chip" Permeability Study and Ex Vivo Optical Imaging, *Int. J. Mol. Sci.*, 2022, **23**, 4237.

28 X. Liu, Y. Zhang, W. Li, B. Zhang, J. Yin, S. Liuqi, J. Wang, B. Peng and S. Wang, Fucoidan Ameliorated Dextran Sulfate Sodium-Induced Ulcerative Colitis by Modulating Gut Microbiota and Bile Acid Metabolism, *J. Agric. Food Chem.*, 2022, **70**, 14864–14876.

29 Y. Peng, Y. Yan, P. Wan, D. Chen, Y. Ding, L. Ran, J. Mi, L. Lu, Z. Zhang, X. Li, X. Zeng and Y. Cao, Gut microbiota modulation and anti-inflammatory properties of anthocyanins from the fruits of Lycium ruthenicum Murray in dextran sodium sulfate-induced colitis in mice, *Free Radicals Biol. Med.*, 2019, **136**, 96–108.

30 L. Xie, T. Chen, X. Qi, H. Li, J. Xie, L. Wang, J. Xie and Z. Huang, Exopolysaccharides from Genistein-Stimulated Monascus purpureus Ameliorate Cyclophosphamide-Induced Intestinal Injury via PI3K/AKT-MAPKs/NF-κB Pathways and Regulation of Gut Microbiota, *J. Agric. Food Chem.*, 2023, **71**, 12986–13002.

31 J. He, C. Wan, X. Li, Z. Zhang, Y. Yang, H. Wang and Y. Qi, Bioactive Components and Potential Mechanism Prediction of Kui Jie Kang against Ulcerative Colitis via Systematic Pharmacology and UPLC-QE-MS Analysis, *Evid. Based Complement. Alternat. Med.*, 2022, **2022**, 9122315.

32 T. Wang, C. Shi, S. Wang, Y. Zhang, S. Wang, M. Ismael, J. Zhang, X. Wang and X. Lü, Protective Effects of Companilactobacillus crustorum MN047 against Dextran Sulfate Sodium-Induced Ulcerative Colitis: A Fecal Microbiota Transplantation Study, *J. Agric. Food Chem.*, 2022, **70**, 1547–1561.

33 Z. Wu, S. Huang, T. Li, N. Li, D. Han, B. Zhang, Z. Z. Xu, S. Zhang, J. Pang, S. Wang, G. Zhang, J. Zhao and J. Wang, Gut microbiota from green tea polyphenol-dosed mice improves intestinal epithelial homeostasis and ameliorates experimental colitis, *Microbiome*, 2021, **9**, 184.

34 K. J. Livak and T. D. Schmittgen, Analysis of Relative Gene Expression Data Using Real-Time Quantitative PCR and the 2−ΔΔCT Method, *Methods*, 2001, **25**, 402–408.

35 N. Hanning, J. Man and B. Winter, Measuring Myeloperoxidase Activity as a Marker of Inflammation in Gut Tissue Samples of Mice and Rat, *Bio-Protoc.*, 2023, **13**, e4758.

36 Y. Wang, H. Tao, H. Huang, Y. Xiao, X. Wu, M. Li, J. Shen, Z. Xiao, Y. Zhao, F. Du, H. Ji, Y. Chen, C. H. Cho, Y. Wang, S. Wang and X. Wu, The dietary supplementRhodiola crenulataextract alleviates dextran sulfate sodium-induced colitis in mice through anti-inflammation, mediating gut barrier integrity and reshaping the gut microbiome, *Food Funct.*, 2021, **12**, 3142–3158.

37 L. Song, Y. Zhang, C. Zhu, X. Ding, L. Yang and H. Yan, Hydrogen-rich water partially alleviate inflammation, oxidative stress and intestinal flora dysbiosis in DSS-induced chronic ulcerative colitis mice, *Adv. Med. Sci.*, 2022, **67**, 29–38.

38 S. Liu, W. Zhao, P. Lan and X. Mou, The microbiome in inflammatory bowel diseases: from pathogenesis to therapy, *Protein Cell*, 2020, **12**, 331–345.

39 A. Martyniak, A. Medyńska-Przęczek, A. Wędrychowicz, S. Skoczeń and P. J. Tomasik, Prebiotics, Probiotics, Synbiotics, Paraprobiotics and Postbiotic Compounds in IBD, *Biomolecules*, 2021, **11**, 1903.

40 M. Liu, J. Ding, H. Zhang, J. Shen, Y. Hao, X. Zhang, W. Qi, X. Luo, T. Zhang and N. Wang, Lactobacillus casei LH23 modulates the immune response and ameliorates DSS-induced colitis via suppressing JNK/p-38 signal pathways and enhancing histone H3K9 acetylation, *Food Funct.*, 2020, **11**, 5473–5485.

41 M. Deng, X. Wu, X. Duan, J. Xu, X. Yang, X. Sheng, P. Lou, C. Shao, C. Lv and Z. Yu, Lactobacillus paracasei L9 improves colitis by expanding butyrate-producing bacteria that inhibit the IL-6/STAT3 signaling pathway, *Food Funct.*, 2021, **12**, 10700–10713.

42 M. T. Alam, G. C. A. Amos, A. R. J. Murphy, S. Murch, E. M. H. Wellington and R. P. Arasaradnam, Microbial imbalance in inflammatory bowel disease patients at different taxonomic levels, *Gut Pathog.*, 2020, **12**, 1–8.

43 I. Verstreken, W. Laleman, G. Wauters and J. Verhaegen, Desulfovibrio desulfuricans Bacteremia in an Immunocompromised Host with a Liver Graft and Ulcerative Colitis, *J. Clin. Microbiol.*, 2012, **50**, 199–201.

44 S. Herp, A. C. Durai Raj, M. Salvado Silva, S. Woelfel and B. Stecher, The human symbiont Mucispirillum schaedleri: causality in health and disease, *Med. Microbiol. Immunol.*, 2021, **210**, 173–179.

45 D. Berry, O. Kuzyk, I. Rauch, S. Heider, C. Schwab, E. Hainzl, T. Decker, M. Müller, B. Strobl, C. Schleper, T. Urich, M. Wagner, L. Kenner and A. Loy, Intestinal Microbiota Signatures Associated with Inflammation History in Mice Experiencing Recurring Colitis, *Front. Microbiol.*, 2015, **6**, 1408.

46 Y. Liu, F. Yin, L. Huang, H. Teng, T. Shen and H. Qin, Long-term and continuous administration of Bacillus subtilis during remission effectively maintains the remission of inflammatory bowel disease by protecting intestinal integrity, regulating epithelial proliferation, and reshaping microbial structure and function, *Food Funct.*, 2021, **12**, 2201–2210.

47 J. Sun, H. Chen, J. Kan, Y. Gou, J. Liu, X. Zhang, X. Wu, S. Tang, R. Sun, C. Qian, N. Zhang, F. Niu and C. Jin, Anti-inflammatory properties and gut microbiota modulation of an alkali-soluble polysaccharide from purple sweet potato in DSS-induced colitis mice, *Int. J. Biol. Macromol.*, 2020, **153**, 708–722.

48 L. Rodes, Effect of Probiotics Lactobacillus and Bifidobacterium on Gut-Derived Lipopolysaccharides and Inflammatory Cytokines: An In Vitro Study Using a Human Colonic Microbiota Model, *J. Microbiol. Biotechnol.*, 2013, **23**, 518–526.

49 P. Huang, X. Wang, S. Wang, Z. Wu, Z. Zhou, G. Shao, C. Ren, M. Kuang, Y. Zhou, A. Jiang, W. Tang, J. Miao, X. Qian, A. Gong and M. Xu, Treatment of inflammatory bowel disease: Potential effect of NMN on intestinal barrier and gut microbiota, *Curr. Res. Food Sci.*, 2022, **5**, 1403–1411.

50 D. Parada Venegas, M. K. De la Fuente, G. Landskron, M. J. González, R. Quera, G. Dijkstra, H. J. M. Harmsen, K. N. Faber and M. A. Hermoso, Short Chain Fatty Acids (SCFAs)-Mediated Gut Epithelial and Immune Regulation and Its Relevance for Inflammatory Bowel Diseases, *Front. Immunol.*, 2019, **10**, 277.

51 O. Kaczmarczyk, A. Dąbek-Drobny, M. Woźniakiewicz, P. Paśko, J. Dobrowolska-Iwanek, A. Woźniakiewicz, A. Targosz, A. Ptak-Belowska, A. Piątek-Guziewicz, K. Wcisło, P. Zagrodzki and M. Zwolińska-Wcisło, Association between fecal levels of Short-Chain Fatty Acids and serum Pro- and Anti-Inflammatory Cytokines in patients with Inflammatory Bowel Disease, *Folia Med. Cracov.*, 2022, **62**, 43–55.

52 S. Sharma, R. Bhatia, K. Devi, A. Rawat, S. Singh, S. K. Bhadada, M. Bishnoi, S. S. Sharma and K. K. Kondepudi, A synbiotic combination of Bifidobacterium longum Bif10 and Bifidobacterium breve Bif11, isomaltooligosaccharides and finger millet arabinoxylan prevents dextran sodium sulphate induced ulcerative colitis in mice, *Int. J. Biol. Macromol.*, 2023, **231**, 123326.

53 C. Yan, S.-H. Huang, H.-F. Ding, E. Kwek, J.-H. Liu, Z.-X. Chen, K. Y. Ma and Z.-Y. Chen, Adverse effect of oxidized cholesterol exposure on colitis is mediated by modulation of gut microbiota, *J. Hazard. Mater.*, 2023, **459**, 132057.

54 X. Bian, W. Wu, L. Yang, L. Lv, Q. Wang, Y. Li, J. Ye, D. Fang, J. Wu, X. Jiang, D. Shi and L. Li, Administration of Akkermansia muciniphila Ameliorates Dextran Sulfate Sodium-Induced Ulcerative Colitis in Mice, *Front. Microbiol.*, 2019, **10**, 2259.

55 Q.-Y. Cui, X.-Y. Tian, X. Liang, Z. Zhang, R. Wang, Y. Zhou, H.-X. Yi, P.-m. Gong, K. Lin, T.-J. Liu and L.-W. Zhang, Bifidobacterium bifidum relieved DSS-induced colitis in mice potentially by activating the aryl hydrocarbon receptor, *Food Funct.*, 2022, **13**, 5115–5123.

56 H. Zhang, J. Xu, Q. Wu, H. Fang, X. Shao, X. Ouyang, Z. He, Y. Deng and C. Chen, Gut Microbiota Mediates the Susceptibility of Mice to Sepsis-Associated Encephalopathy by Butyric Acid, *J. Inflammation Res.*, 2022, **15**, 2103–2119.

57 N. Schlegel, K. Boerner and J. Waschke, Targeting desmosomal adhesion and signalling for intestinal barrier stabilization in inflammatory bowel diseases—Lessons from experimental models and patients, *Acta Physiol.*, 2020, **231**, e13492.

58 X. Dou, L. Qiao, J. Chang, S. Yan, X. Song, Y. Chen, Q. Xu and C. Xu, Lactobacillus casei ATCC 393 and it's metabolites alleviate dextran sulphate sodium-induced ulcerative colitis in mice through the NLRP3-(Caspase-1)/IL-1β pathway, *Food Funct.*, 2021, **12**, 12022–12035.

59 X. Cai, Y. Han, M. Gu, M. Song, X. Wu, Z. Li, F. Li, T. Goulette and H. Xiao, Dietary cranberry suppressed colonic inflammation and alleviated gut microbiota dysbiosis in dextran sodium sulfate-treated mice, *Food Funct.*, 2019, **10**, 6331–6341.

60 J. Wang, H. Chen, B. Yang, Z. Gu, H. Zhang, W. Chen and Y. Q. Chen, Lactobacillus plantarum ZS2058 produces CLA to ameliorate DSS-induced acute colitis in mice, *RSC Adv.*, 2016, **6**, 14457–14464.

61 Y. Zhang, X. Feng, H. Lin, X. Chen, P. He, Y. Wang and Q. Chu, Tieguanyin extracts ameliorated DSS-induced mouse colitis by suppressing inflammation and regulating intestinal microbiota, *Food Funct.*, 2022, **13**, 13040–13051.